Multifaceted enrichment analysis of RNA–RNA crosstalk reveals cooperating micro-societies in human colorectal cancer

Tommaso Mazza[1],[*],[†], Gianluigi Mazzoccoli[2],[*],[†], Caterina Fusilli[1], Daniele Capocefalo[1], Anna Panza[3], Tommaso Biagini[1], Stefano Castellana[1], Annamaria Gentile[3], Angelo De Cata[2], Orazio Palumbo[4], Raffaella Stallone[4], Rosa Rubino[2], Massimo Carella[4] and Ada Piepoli[5],[*]

[1]Bioinformatics Unit, IRCCS Scientific Institute and Regional General Hospital 'Casa Sollievo della Sofferenza', San Giovanni Rotondo (FG), Italy, [2]Department of Medical Sciences, Division of Internal Medicine and Chronobiology Unit, IRCCS Scientific Institute and Regional General Hospital 'Casa Sollievo della Sofferenza', San Giovanni Rotondo (FG), Italy, [3]Department of Medical Sciences, Division of Gastroenterology and Research Laboratory, IRCCS Scientific Institute and Regional General Hospital 'Casa Sollievo della Sofferenza', San Giovanni Rotondo (FG), Italy, [4]Medical Genetics, IRCCS Scientific Institute and Regional General Hospital 'Casa Sollievo della Sofferenza', San Giovanni Rotondo (FG), Italy and [5]Division of Epidemiology and Health Statistics, IRCCS Scientific Institute and Regional General Hospital 'Casa Sollievo della Sofferenza', San Giovanni Rotondo (FG), Italy

ABSTRACT

Alterations in the balance of mRNA and microRNA (miRNA) expression profiles contribute to the onset and development of colorectal cancer. The regulatory functions of individual miRNA-gene pairs are widely acknowledged, but group effects are largely unexplored. We performed an integrative analysis of mRNA–miRNA and miRNA–miRNA interactions using high-throughput mRNA and miRNA expression profiles obtained from matched specimens of human colorectal cancer tissue and adjacent non-tumorous mucosa. This investigation resulted in a hypernetwork-based model, whose functional backbone was fulfilled by tight micro-societies of miRNAs. These proved to modulate several genes that are known to control a set of significantly enriched cancer-enhancer and cancer-protection biological processes, and that an array of upstream regulatory analyses demonstrated to be dependent on miR-145, a cell cycle and MAPK signaling cascade master regulator. In conclusion, we reveal miRNA-gene clusters and gene families with close functional relationships and highlight the role of miR-145 as potent upstream regulator of a complex RNA–RNA crosstalk, which mechanistically modulates several signaling pathways and regulatory circuits that when deranged are relevant to the changes occurring in colorectal carcinogenesis.

INTRODUCTION

An important paradigm of RNA–RNA interaction is operated by a class of small non-coding RNAs called microRNAs (miRNAs or miRs), which are involved in the post-transcriptional regulation of RNA transcripts, by base-pairing to partially complementary sites on the target messenger RNAs (mRNAs), usually in the 3′ untranslated region (3′ UTR). Each miRNA has the potential to target many genes, with many miRNAs able to synergistically regulate the same mRNA transcript (1,2).

Alterations in non-coding transcripts may play important roles in cancer pathogenesis. Numerous miRNA-encoding genes are frequently located at fragile genomic sites or within regions frequently deleted or amplified in neoplastic diseases (3). Deletion, mutation or methylation of miRNA-encoding genes may cause deregulated expression of critical miRNAs, which can then act as oncomiRs or tumour suppressors (4).

The main hallmark of colorectal carcinogenesis is the accumulation of genetic alterations in oncogenes and tumour suppressor genes, which control crucial cellular processes

such as proliferation, differentiation and apoptosis in the colorectal epithelium (5). The first group of genetic alterations includes inducers of chromosomal instability, which is driven by amplifications/deletions of whole or subsections of chromosomes that can underlie both the progressive inactivation of tumour suppressor genes, such as adenomatous polyposis coli (*APC*), deleted in colorectal cancer *SMAD4* and *TP53*, and the activation of oncogenes such as *KRAS* (6,7). The second group of genetic alterations induces microsatellite instability (MSI), which is associated with mutations in genes containing simple repeats, such as those encoding the epidermal growth factor receptor (*EGFR*), the apoptotic factor BCL2-associated X protein (*BAX*) and the transforming growth factor β receptor II (*TGFBR2*). MSI results in the inactivation of genes belonging to the DNA mismatch repair family (8,9). The third group of genetic alterations includes epigenetic alterations, which together make the so said CpG island methylator phenotype (CIMP). CIMP is characterized by epigenetic instability and by high methylation levels of the promoters of some tumour suppressor genes, such as the Cyclin-Dependent Kinase Inhibitor 2A (*CDKN2/p16*), insulin-like growth factor 2 (*IGF2*) and *MLH1* (10).

All these events impact several key signaling pathways that are commonly deregulated in carcinogenesis, including WNT-β-catenin, EGFR, mitogen-activated protein kinase (MAPK), TGF-β and phosphatidylinositol 3-kinase (PI3K). Alterations in the WNT-β-catenin pathway are responsible for many epithelial tumours, being involved in approximately 30–70% of human sporadic colorectal cancers (CRCs). Mutations in the *APC* gene, affecting the carboxy-terminal region, are implicated in β-Catenin and axin binding, leading to the deregulated nuclear translocation of the β-catenin transcription factor from the cytoplasm (11). This induces the genesis of a tumour phenotype by enhancing the transcription of a number of oncogenes and target genes, such as *MYC* and *CCND1* (12). Sporadic CRCs, negative for *APC* or *CTNNB1* gene mutations, are characterized by activation of the WNT signaling pathway via *APC* inhibition by miR-135, which, in turn, is upregulated in CRC, or by direct modulation of β-catenin by miR-200a, which alternatively interacts with the 3' UTR of *CTNNB1* or drives the down-regulation of the *ZEB1/2* gene (13). EGFR is an important player in colorectal carcinogenesis, being a modulator of critical cellular processes such as proliferation, adhesion and migration. The EGFR intracellular signal transduction pathways include components of the MAPK, PI3K, signal transducer and activator of transcription, protein kinase C and phospholipase D pathways. In particular, the MAPK pathway modulates numerous key kinases, which, in turn, control cell growth, differentiation, proliferation, apoptosis and migration through a series of intermediate proteins, including *RAF*, *MEK* and *RAS* (14). The latter is a critical gene, since it can unleash its signaling cascade either by PI3K, thereby inhibiting apoptosis, or by RAF, thereby stimulating cellular proliferation. The anomalous activation of the receptor tyrosine kinases or the gain-of-function mutations occurring in the *RAS* or *RAF* genes are reported to cause the deregulation of the RAS-RAF-MEK-ERK-MAPK axis, which, in turn, is a frequent therapeutic target (15–17). Interestingly, the down-regulation of miR-

143 was shown to contribute to *ERK/MAPK* activation, as well as to *KRAS* and *ERK5* repression (18).

CRC onset and progression are related to a combination of causal perturbations occurring at any *omics* layer (19) and relevant studies have brought out the anomalous interactions between gene transcripts and miRNA molecules as crucial causes of carcinogenesis (20–24). In exactly this direction, this work aims at scrutinizing the mRNA–miRNA crosstalks in search of mutual and combined effects on the whole colorectal carcinogenesis process. It borrowed computational and analytical methods from Systems Biology to inspect both transcriptome layers and their interactions, and to look for socially central (groups of) molecules. We addressed this issue by a multifaceted analysis strategy, encompassing a series of functional enrichment, topological and clustering analyses, which were conducted on genome-wide mRNA and miRNA expression profiles of matched pairs of tumour and adjacent non-tumorous mucosa samples obtained from CRC patients. *In silico* analyses highlighted the prominent topological position of miRNA-145, and its mechanistic role in maintaining cohesiveness and functional cooperation among groups of key miRNAs and genes. Given the critical tumour suppressive role of miR-145, its action, combined with several other miRs, was deemed responsible for a coordinated program of patterned gene regulation, whose master regulator was actually miR-145. The discovery of its partners and of the unexplored effects of their interactions in colorectal carcinogenesis was, therefore, a further objective of this work. This was achieved by first identifying *in silico* the co-expressing partners of miR-145, and then, by perturbing them *in vitro* in four CRC cell lines. We verified that the ectopic expression of miR-145 impacts the whole miRNA network and that, downstream, this perturbs the MAPK signaling cascade.

MATERIALS AND METHODS

Data sources

The datasets analysed in this study consisted of the transcriptome (25) and miRNAome (20) of a set of 14 matched pairs of tumour and adjacent non-tumorous mucosa samples obtained from CRC patients and evaluated with the GeneChip Human Exon 1.0 ST array and GeneChip miRNA 2.0 array (Affymetrix, Santa Clara, CA, USA).

Statistical analysis

Expression data analyses were performed using GNU R ver. 3.0.2 (http://www.r-project.org/) and the Partek Genomics Suite package ver. 6.6 (Partek, St. Louis, MO, USA). Low-level analysis and normalization were done using GCRMA (26) and Partek. We filtered the probe sets and kept only those present in at least six samples. To reduce noise, we also removed probe sets that do not map to an Entrez gene. Batch effects were removed by the Partek's batch effect removal algorithm. The resulting genes and miRs were tested for differential expression, using the paired *t*-statistics. Under the assumption of equal variance between groups, allowing a number of false positives equals to 2% of the genome and setting the minimum $\log_2$ fold change ($\log_2$ FC) expression barriers to ± 1.5, we achieved a statistical

power of 0.8. Correlations between miRNA expression values were estimated using the Spearman's rank correlation coefficient (r_s) using Rcmdr (27). (i) The relationships between miR-145 and its direct and indirect partners were ascertained by regression analysis. Time-to-event analysis was performed by the Mantel-Haenszel test and the 50% percentiles of miRNAs were used to dichotomize patients into low and high expression groups. Kaplan–Meier curves were drawn for CRC patients taken from The Cancer Genome Atlas (TCGA) dataset (https://tcga-data.nci.nih.gov/tcga/tcgaHome2.jsp). A *P*-value <0.05 was considered statistically significant. Equality of proportion was assessed by Chi-squared test.

Gene selection strategy and *in silico* functional and pathway analyses

To make results more reliable, only differentially expressed genes deregulated in at least five CRC-related experiments retrieved from Gene Expression Atlas (28) were selected. These underwent functional enrichment analysis against the Gene Ontology FAT sub-set and the set of genes with probe sets included in the used Affymetrix chips. Results obtained with DAVID (29) web services were cross-checked with Babelomics (30) and considered for inclusion if Bonferroni-corrected significance levels did not exceed 5%. General functional classes were refined by a mixture test between the *elim* and *weight* algorithms (31). These determined the best enrichment in a bottom-up order, by progressively removing genes from functional classes, which were enriched by more specific categories. This analytical procedure facilitated the identification of specific *cancer-favorable* and *cancer-protection* processes, with statistical confidence. Pathways were detected by ToppGene (32), where the hypergeometric distribution with False Discovery Rate (FDR) correction was used as the standard method for determining statistical significance. The *P*-value cut-off was set to 0.05, while the *gene limits* ranged from 1 to 1500.

MiRNA selection strategy

We obtained a list of miRs that are reliably associated with CRC by intersecting the set of miRs reported by miRSystem (33) to target the genes selected in the previous analytical steps with that of miRs associated to CRC, according to the Human microRNA disease Database (HMDD) (34). MiRSystem is a database that integrates seven well-known target gene prediction programs: DIANA, miRanda, miRBridge, PicTar, PITA, rna22 and TargetScan. The observed identification probability (O) for a given gene is the proportion of the queried miRNAs predicted to target that gene, whereas the expected probability (*E*) is the proportion of all miRNAs in the miRSystem database predicted to target that gene, i.e. the number of target gene-miRNA pairs deposited in the miRSystem database. This expected probability represents the chance of one gene being randomly selected by miRNAs. We only considered experimentally validated targets, with an O/E ratio greater than 1.5.

Networks analysis

We obtained hypergraphs connecting genes by querying a number of heterogeneous data sources: (i) Interpro and PFAM, (ii) Gene Expression Omnibus, (iii) BIOGRID and IREF, (iv) PathwayCommons, IMID, NCI-NATURE, REACTOME, KEGG, BIOCARTA and (v) BIOGRID, BIND, HPRD, INTACT, MINT, MPPI, OPHID, through GeneMANIA (35). We linked any two genes by an undirected edge, whenever an evidence of interaction was found, which we weighted with a value provided by GeneMANIA that indicates the predictive power of the selected dataset for that edge (35). Several pairs of genes could be connected by more than one edge. In such case, we agglomerated the weights of multiple edges by the injective function

$$W_{AB} = \frac{e^n}{n} \sum_{i=1}^{n} W_{AB_i},$$

where *n* is the number of edges connecting any two nodes *A* and *B*, and *i* refers to the *i*th edge. W_{ABi} stands for the weight of the *i*th edge. The multiplicative factor $\frac{e^n}{n}$ is meant to give increasing importance to multiple links in respect to isolated links (36). We then built weighted graphs with weights over the edges (carrying the reliability of the corresponding interactions).

MiRNAs were given in input to Ingenuity Pathway Analysis (IPA), which wired a relevant network based on extensive records maintained in the Ingenuity Pathways Knowledge Base. This knowledge base has been abstracted into a large network, called the Global Molecular Network, composed of thousands of molecules that interact with each other. Two molecules (miRNAs and genes here) are connected if there is a path in the network between them. Interactions can be physical and functional. We considered only physical interactions and cancer-related functions, to build a *literature-based* network. Dashed edges stand for indirect relationships between molecules, i.e. they summarize paths longer than one step.

The same set of miRNAs was filtered to contain only those that were differentially expressed between our CRC and control tissues as well as those that exhibited any significant correlation of expression with at least another miRNA (*P*-value < 0.05, $r_s > 0.4$ or $r_s < -0.4$). The resulting miRNAs were linked with non-oriented edges, since correlation is a symmetric measure, and weighted using the Spearman's rank correlation coefficient (r_s), to make an e*xperimental* network (20).

Topological analysis

Genes and miRNAs were assigned a topological importance. All the considered metrics were based on the enumeration of links (or *shortest paths*). Considering a path from *s* ∈ *V* to *t* ∈ *V*, with *V* the set of nodes, as an alternating sequence of nodes and edges beginning with *s* and ending with *t*, such that each edge connects its preceding with its succeeding node, we calculated the length of a path by summing the inverse weights of its edges. The idea is that highly correlated miRNAs or functionally closest genes minimize their distance. We calculated *degree*, *betweenness*, *closeness, radiality* and *clustering coefficient* centrality indices, and ranked

miRNAs and genes accordingly. Definitions of these indices have been detailed previously (20).

Privileged topological position of miRs were inferred by a combination of the IPA's tools: BioProfiler and Upstream Regulatory Analysis. These allowed inferring both which miRNAs might have been up- or down-regulated in the experiment and which one might be causally relevant. Activation z-scores were conservatively kept to a minimum of ±2.

Networks were drawn and analysed both by a custom standalone tool, written in C# and using NodeXL 1.0.1.332 (37), and by Cytoscape 3.0 (38).

Strongly connected components

Functional affinities of genes and miRNAs were sought among highly cohesive groups of genes and miRNAs. To this end, we used the *Cluster ONE* algorithm (39). It handles weighted graphs and generates overlapping clusters. It starts from a single node and greedily adds or removes new nodes, if they alter the cohesiveness of the group. Subgroups of less than five nodes or having a density less than a given threshold (set at 3) were discarded. Finally, redundant cohesive subgroups were merged to form larger subgroups to make the results easier to interpret.

MiRNAome and MAPK signaling pathway profiling after miR-145 transfection in colon cancer cell lines

To identify any functional synergistic pairs of miRNAs, the global miRNA expression profile was obtained in the transfected colon cancer cell lines, as previously reported (20). Briefly, CaCo2, SW480, HCT116 and HT-29 cell lines were transiently transfected using HiPerfect Transfection Reagent (QIAGEN), with synthetic miR-145 mimic (MSY0000437, QIAGEN), following the manufacturer's instructions, as previously described (40). The total RNA was purified using the RNeasy kit (QIAGEN) and labelled using the 3DNA Array Detection FlashTagTM RNA Labeling Kit (www.genisphere.com). Samples were hybridized on Gene-Chip miRNA Array (www.affymetrix.com), washed and scanned with an Affymetrix Scanner. MiRNA expression data were then processed and analysed using the Robust Multi-array Average algorithm, and deposited in the EMBL-EBI Array Express.

To assess the effect exerted by miR-145 on the MAPK signaling pathway, gene expression levels of the transfected cell lines were quantified by using RT^2 MAP Kinase Signaling Pathway PCR Arrays (SABiosciences). Briefly, mRNA and cDNA were prepared using reagents and equipment from QIAGEN (QIAGEN Hamburg, Germany) and assayed with the RT^2 MAP Kinase Signaling Pathway PCR Arrays (SABiosciences) with SABiosciences RT^2 qPCR Master Mix according to the manufacturer's instructions. Plates were read on 7900 TaqMan (Applied BioSystem, Life Technologies Corporation) with 1 cycle of 10 min at 95°C followed by 45 cycles of 15 s at 95°C and 1 min at 60°C. SYBR Green fluorescence was monitored at the annealing step of each cycle and analysed with SDS v.2.4 software (Applied BioSystem, Life Technologies Corporation). The analysis of the gene expression was completed using the SA Bio-

sciences PCR Array Data Analysis Web Portal, as recommended by the manufacturer, and verified using the $\Delta\Delta Ct$ method.

RESULTS

From biological processes to gene regulatory networks

A total of 4.441 genes were significantly deregulated between matched tumour and adjacent non-tumorous tissues (2.549 up-regulated and 1.892 down-regulated in the CRC specimens), of which 1.645 and 878, respectively, maintained the same expression direction in at least five experiments deposited in the EBI Gene Expression ATLAS. As a proof of concept, we verified that the CRC pathway (*hsa05210* KEGG pathway, Figure 1) was significantly impacted. Twenty-eight out of 45 genes of this pathway were deregulated in a statistically significant way (p =1.32E-10). These genes are known to functionally participate to four macro biological processes (BPs): *proliferation, (anti)-apoptosis, growth* and *cell cycle control.*

Through functional enrichment analysis, 2.091 genes (83% of the whole genes set) significantly associated to at least one of these BPs, compared to 9.089 genes (52.1% of the background set of genes) known to carry out these processes ($P < 0.0001$). Based on the log-Odds ratios and the class of BPs, the resulting BPs were classified as *cancer-favorable* (Adj p =0.016) or *cancer-protection* (Adj p =0.0012), according to whether they were positively or negatively associated to the colorectal carcinogenesis process or, more generally, to *cancer-related* processes (Adj P < 0.001) (Supplementary Table S1). In particular, *cancer-favorable* processes included 48 genes hampering apoptosis, 23 genes promoting cell cycle progression, 92 genes increasing proliferation and 9 genes promoting cell growth. On the other hand, we counted 106 apoptosis-favorable genes, 53 genes promoting cell cycle control, 95 genes hindering proliferation and 24 genes decreasing cell growth. The remaining genes fell in the *cancer-related* set of BPs, 158 of which were apoptosis-associated, 105 involved in cell cycle regulation, 199 were proliferation modulators and 42 were related to cell growth. We selected 391 genes (Supplementary File S1).

We submitted the whole set of 391 genes to GeneMANIA in order to reconstruct their interaction network. Pairs of genes were linked if they shared at least one experimentally verified relationship. The resulting network exhibited relationships of co-expression (52.65% of the total number of relationships), co-localization (14.85%), physical interactions (13.52%), shared pathways (9.06%), shared predicted interactions (8.44%), shared genetic interactions (1.23%) and shared protein domains (0.26%). Technically, this network comes as a hypergraph, since it allows more than one edge connecting two nodes. The network was reduced to a graph, as described in the 'Materials and Methods' section.

The resulting network is made of one connected component, with mild cohesiveness: clustering coefficient = 0.257, diameter = 4 and network density = 0.095. As generally defined, network density ranges from 0 to 1, and measures how densely a network is populated with edges. A network with no edges and solely isolated nodes has a density equal to 0 (cf. Supplementary File S2 for gene-wise topological
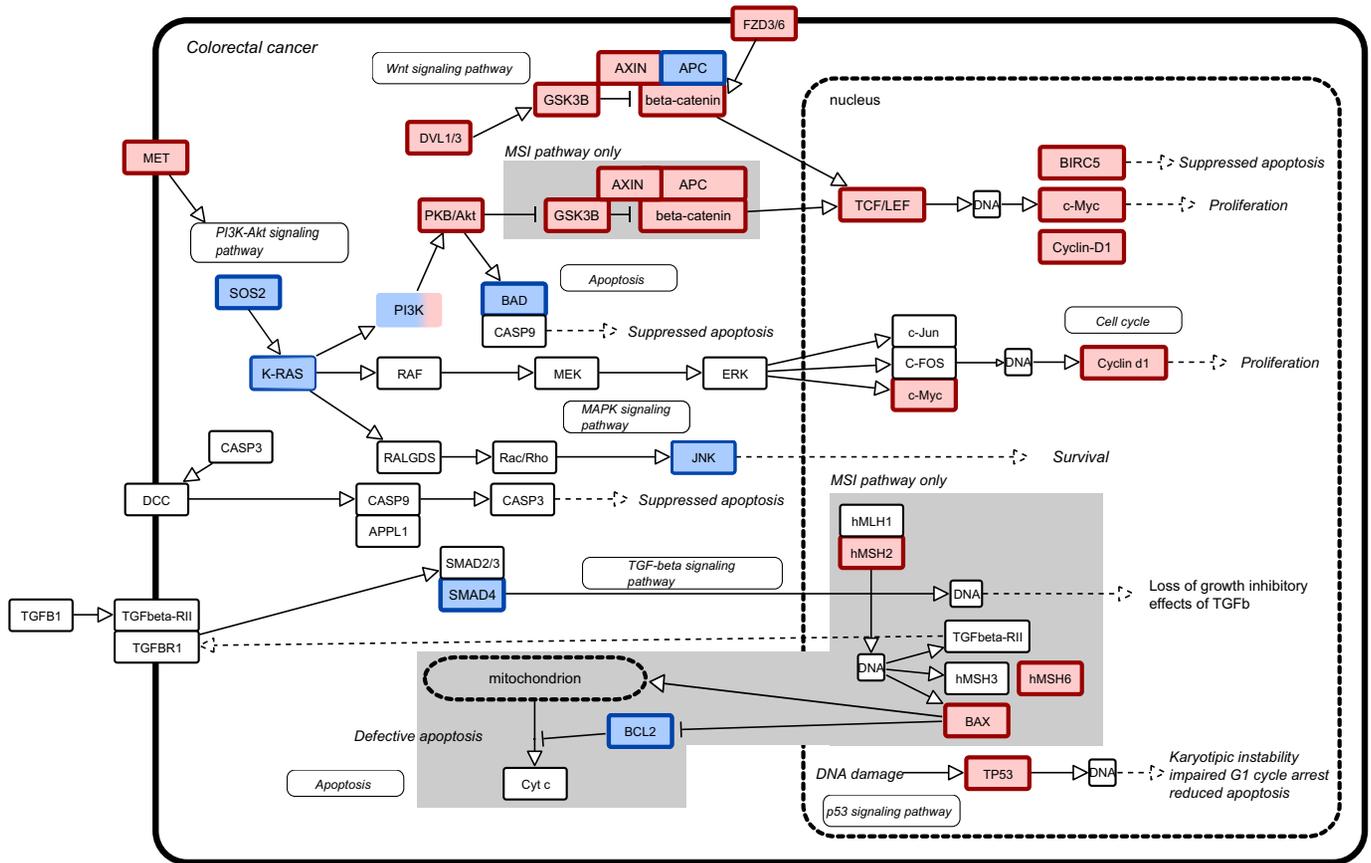
Figure 1. Genes involved in CRC pathway. Up-regulated (red) and down-regulated genes (blue) of the CRC pathway (KEGG id: hsa05210). *TCF7* and *LEF1* glyphs are condensed in *TCF/LEF*; *PIK3R2, PIK3CG, PIK3CD* in *PI3K* and *MAPK10* in *JNK*, being *JNK3* one of its synonyms. As to *PI3K* bicolour representation, *PIK3R2*, was up-regulated, while *PIK3CG* and *PIK3CD* were down-regulated in tumour tissues.

scores). The network decomposition procedure identified 11 modules (Figure 2, Supplementary Table S2), classified and divided into two *cancer-protection* and nine *cancer-favorable* modules, according to the BPs which their genes participate in, and as to whether their genes are up-regulated or down-regulated (Supplementary Table S2). In Supplementary File S2, we report a list of the most central genes, also known as *intramodular hubs*, which includes *TP53* (module 6), *MYC* (module 10), *CDK4* (module 2), *CTNNB1* (module 4), *CHEK1* and *CDK2* (module 1). These were the top six genes, in terms of centrality, for at least three out of the four above-mentioned topology indices. *Intramodular hubs* link to several proteins that are highly self-connected and that are, therefore, more likely to perform any biological task in cooperation (41). Such hubs are almost never pleiotropic.
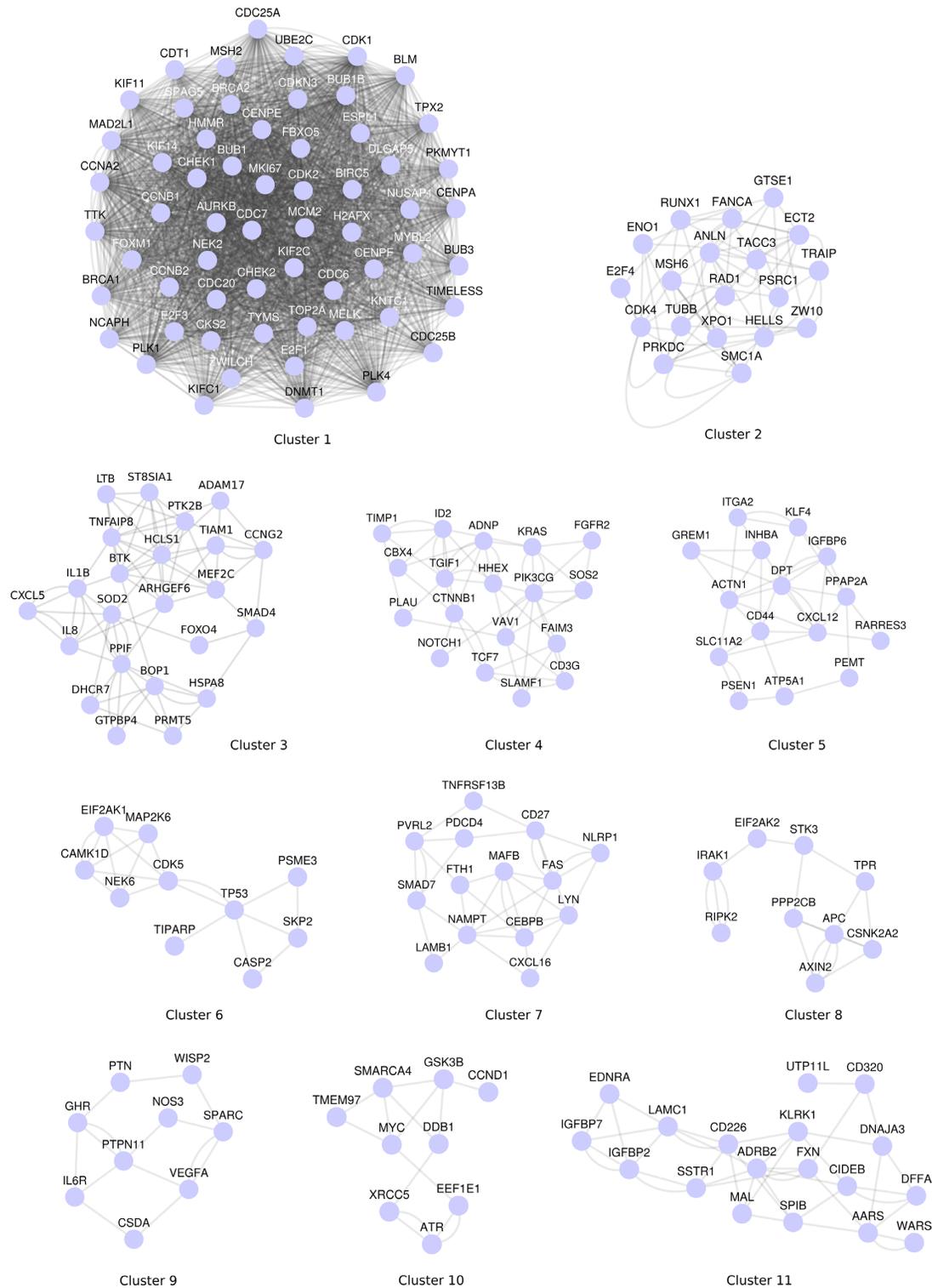
Functional modules in *literature-based* and *experimental* miRNA networks

We have retrieved 41 experimentally verified miRNAs (cf. Supplementary Table S4) targeting the 391 above-mentioned genes by *miRSystem* and selected only those that were reported by the HMDD to be associated to CRC. These were given in input to IPA that wired a *literature-based* network of 19 of these miRNAs, together

with 19 miRNA-controlled genes (Figure 3A). As anticipated, edges among molecules were drawn only if they represented physical interactions or evidence of participation to the same *cancer-related* biological functions.

An *experimental* network was derived from the 41 above-mentioned miRNAs. A miRNA was selected to populate the network only if it was differentially expressed between tumour and adjacent non-tumorous tissues and significantly correlated with at least a miRNA within the network. Thirty-nine out of 41 miRNAs were linked by 148 edges (Figure 3B). Missed miRNAs in the *experimental* and *literature-based* networks are reported in Supplementary Table S4. In particular, the latter network contained miR-335, which was missing in the former. Generally, the *experimental* network almost included the other network. As for the relationships between miRNAs, the two networks did not properly match, indicating that there is room for developing plausible new functional relationships between miRNAs involved in CRC development.

Topological analysis of the *experimental* network indicated two significant clusters: a triangle made of miR-708, miR-18b and miR-17 and a clique made of miR-144, miR-1246, miR-1275 and miR-99a. Both modules were made of nodes not present in the *literature-based* network, but miR-17. MiR-17 and miR-1246 or miR-99a were used as seeding nodes by Cluster ONE for the detection of the modules.

Figure 2. Networks clustering. Nodes represent genes that are connected by undirected edges. Genes may be connected by multiple edges, in cases where more than one functional evidence of interaction exists between them.

Figure 3. *Literature-based* and *experimental* networks of miRNA interactions. (**A**) *Literature-based* network: two miRNAs are connected if there is any evidence of physical or (cancer-related) functional interactions. (**B**) *Experimental* network: it connects any two miRNAs if they are differentially expressed between matched pairs of tumour and adjacent non-tumourous mucosa samples, and if their expression values are statistically correlated. Colours indicate miRNA clusters. Coloured labels specify miRNAs that are topologically important. Red lines join miRNAs making a triangle and a clique.

Figure 4. MiRNAs–mRNAs intermodular hubs. The triangle made of miR-708, miR-18b, miR-17 and the clique made of miR-144, miR-1246, miR-1275, miR-99 interact with four *intermodular hubs*, i.e. *TP53, CDK2, CDK4* and *MYC*.

Among these, miR-708, miR-18a, miR-18b and miR-17, together with miR-92b, miR-10b and let-7e were the most important miRNAs of the network, from a positional perspective (cf. Supplementary File S3). These miRNAs control four of six *intramodular hubs*, namely *TP53, MYC, CDK4* and *CDK2* (cf. Supplementary File S2), which, in this context, can be considered as *intermodular hubs*, as they connect the two modules (Figure 4). It is worth noting that *inter-*

modular hubs are usually pleiotropic and connect to different biological modules, interacting with different partners at different moments and/or within different cellular compartments. As seen in Supplementary Table S3, these miR-NAs also control the top five genes in terms of O/E scores: *CCNA2* (module 1), *MYC* (module 10), *LRP5* (module 8), *E2F1* (module 1), *HSPA8* (module 3), from the initial list of 391 genes.

Leading topological position of miRNA-145 in upholding cohesiveness and functional cooperation among groups

Upstream analysis of intra/intermodular hub genes revealed a prominent mechanistic and topological position of miR-145 (z-score = 2.35), miR-9 (z-score 2.11) and miR-137 (z-score = 2.07). Of these, miR-145 was the only differentially expressed miRNA in our experiment.

The hypothesis that miR-145 could be a master regulator of the CRC network was sustained both statistically, by the *experimental* network, and functionally, by the *literature-based* network. MiR-145 was strongly correlated with most of the aforesaid miRNAs (see Figure 3B). The analysis of gene expression profiles of CRC patients available through the TCGA databank not only confirmed that the expression of miR-145 correlates with that of miR-17, miR-23b and miR-99a (one of the seeding nodes) but also that these were likely to be causally dependent on miR-145 ($P < 0.0001$). Additionally, high expression values of let-7e and miR-92b resulted moderate risk factors, if coupled with high expression values of miR-145. Similarly, low profiles of let-7e and miR-92b conferred a worse prognosis, if coupled with low expression values of miR-145. High values of miR-10b and

miR-143, instead, were risk factors if concomitant with low values of miR-145 (Supplementary File S6).

More generally, miR-145 resulted to be directly connected with several components of important clusters of miRNAs, which in turn targeted relevant intra/inter-modular hub genes, as reported in Supplementary Table S3. Topologically, miR-145 was linked through miR-93 to the triangle made of miR-708, miR-18b and miR-17 and to the clique made of miR-144, miR-1246, miR-1275 and miR-99a, thereby controlling, even indirectly, four *intramodular hubs*, namely *TP53, MYC, CDK4* and *CDK2* (Supplementary File S2).

With no intention of discussing the renowned direct implication of miR-145 deregulation in colorectal carcinogenesis, well aware that molecular competition represents a universal and frequent form of gene regulation that operates also in RNA regulatory networks, and as a consequence of the above results, we focused on the short-range interactions of miR-145 with the aim to highlight its apical regulative role on key genes and biological functions related to CRC development.

Effects of the ectopic expression of miR-145 in CRC cell lines

The effect of the ectopic expression of miR-145 on 866 miR-NAs was assessed in four human colon cancer cell lines. Only miRNAs showing statistically significant differential expression ($P < 0.05$, $\log_2 \text{FC} \geq 1.5$, $\log_2 \text{FC} \leq -1.5$) after miR-145 ectopic expression were considered (see Supplementary File S4). Several miRNAs were differentially expressed in the four tested cell lines: 82 miRNAs in the CaCo2 cell line (32 up-regulated and 50 down-regulated), 120 miRNAs in HT-29 cells (58 up-regulated and 62 down-regulated), 90 miRNAs in HCT116 cells (49 up-regulated and 41 down-regulated) and 95 miRNAs in the SW480 cell line (58 up-regulated and 37 down-regulated). Among these, three direct partners of miR-145 were modulated in three of four cell lines. In particular, miR-99a was highly down-regulated in CaCo2 cells ($p = 0.036$, $\log_2 \text{FC} = -4.36$), miR-23b was mildly down-regulated in the HT29 cell line ($p = 0.004$, $\log_2 \text{FC} = -1.81$), and miR-143 was up-regulated in SW480 cells ($p = 0.046$, $\log_2 \text{FC} = 1.52$). Moreover, among the deregulated miRNAs, we found at least one miRNA, for each cell line, that was indirectly connected to the miR-145: miR-23a ($p = 0.004$, $\log_2 \text{FC} = -5.14$) in CaCo2 cells; miR-23a ($p = 0.008$, $\log_2 \text{FC} = -1.84$) and miR-27a ($p = 0.039$, $\log_2 \text{FC} = -2.5$) in HT29 cell, with both included in miR23a∼miR27a∼miR24-2 cluster, and being down-regulated; miR-18a* ($p = 0.002$, $\log_2 \text{FC} = 2.32$), included in the miR17∼miR92a cluster, and miR-24-1* ($P < 0.001$, $\log_2 \text{FC} = 2.4$), included in miR23b∼miR27b∼miR3074 cluster, were up-regulated in SW480 cells. MiR-1246 was also up-regulated in HCT-116 cells ($p = 0.041$, $\log_2 \text{FC} = 3.47$) and mildly in HT29 cells ($p = 0.038$, $\log_2 \text{FC} = 1.32$).

All direct and indirect targets of miR-145 that resulted from our *in silico* analysis, other than enriching several cell-cycle related processes, did significantly enrich two important pathways: the PI3K pathway through *FGF3, FRAP1* and *RPTOR* ($p = 0.000049$), the WNT signaling pathway through *FZD5, FZD8* and *PPP3CA* ($p = 0.00039$), and the MAPK signaling pathway through *CRK, FAS,*

MAP3K5, MAP3K8, MAPK14, RAPGEF2, RPS6KA5, TGFBR2, CHUK, DUSP5, MAP4K3, PDGFA, RRAS2, DUSP8, FGF4, HSPA8, FGFR3, FRAP1 and *PPP3CA* genes ($p = 0.0289$).

MAPK signaling pathway is modulated by miR-145 ectopic expression in CRC cell lines

The main impact of miR-145 over-expression regarded the expression of several genes participating to the MAPK signaling pathway. Their expression profiles were compared with those measured in untransfected cells, as well as in matched tumorous and adjacent non-tumorous colon tissues obtained from CRC patients (Figure 5).

In particular, *CDKN2C* greatly increased its expression both in CaCo2 and in HT-29 cells ($\log_2 \text{FC} = 3.43$ and 4.46, respectively), while it was not differentially expressed in the genome-wide profiling study. On the other hand, *MAP2K4* slightly increased its expression in both HCT116 and HT-29 cells ($\log_2 \text{FC} = 1.69$ and 1.37, respectively), whereas it was significantly down-regulated in the tumour tissues ($\log_2 \text{FC} = -2.87$). A similar trend was observed in HT29 cells for the following genes: *CDKN1A, CDKN2B, KRAS, PRDX6* and *SMAD4. KRAS* and *SMAD4* that were up-regulated after transfection ($\log_2 \text{FC} = 1.53$ and 2.74, respectively), but were down-regulated in our CRC specimens ($\log_2 \text{FC} = -2.63$ and -3.1, respectively). Finally, *ELK1* and *CDK2*, which exhibited elevate *closeness* and *degree* centrality scores, were both up-regulated in our CRC specimens ($\log_2 \text{FC} = 4.56$ and 4.34, respectively). In contrast, *ELK1* was down-regulated in HCT116 cells ($\log_2 \text{FC} = -4.64$) and up-regulated in HT-29 cells ($\log_2 \text{FC} = 1.93$), while *CDK2* was imperceptibly down-regulated in SW480 cells ($\log_2 \text{FC} = -1.17$) and up-regulated in HT-29 cells ($\log_2 \text{FC} = 2.27$), after miR-145 transfection (Figure 5 and Supplementary File S5). Interestingly, HT29 cells showed up-regulation of most of the MAPK pathway genes, with the exception of *CDKN1C, LAMTOR3* and *RLPO*.

These genes are not direct targets of miR-145, but of miR23a, miR-23b, miR-26b, miR-99a and miR-18a (Supplementary Table S5), which in turn, were deregulated in the four cell lines, as an effect of the ectopic expression of miR-145 (Supplementary File S4). In particular, we found alterations of both miR-23a and miR-23b in HT-29 cells. Being highly similar in their mature sequences, they are expected to control the same transcripts, which are known to mostly belong to the KRAS and TGFβ signaling pathways, and which, in our study, are those of the *K-RAS, cMYC* and *E2F1* genes, as reported in Figure 6.

DISCUSSION

Our integrative analysis of mRNA–miRNA and miRNA–miRNA interactions identified two *cancer-protection* and nine *cancer-favorable* modules of genes and provided interesting mRNA–miRNA crosstalks. A number of genes emerged that demonstrated a relevant dual role, both being *intramodular* and *intermodular* hubs. A strongly connected sub-network was made up, in fact, by *TP53, MYC, CDK4, CTNNB1, CHEK1* and *CDK2*, which were the most central genes (some of the *intramodular hubs*). *CDK4, CDK2*
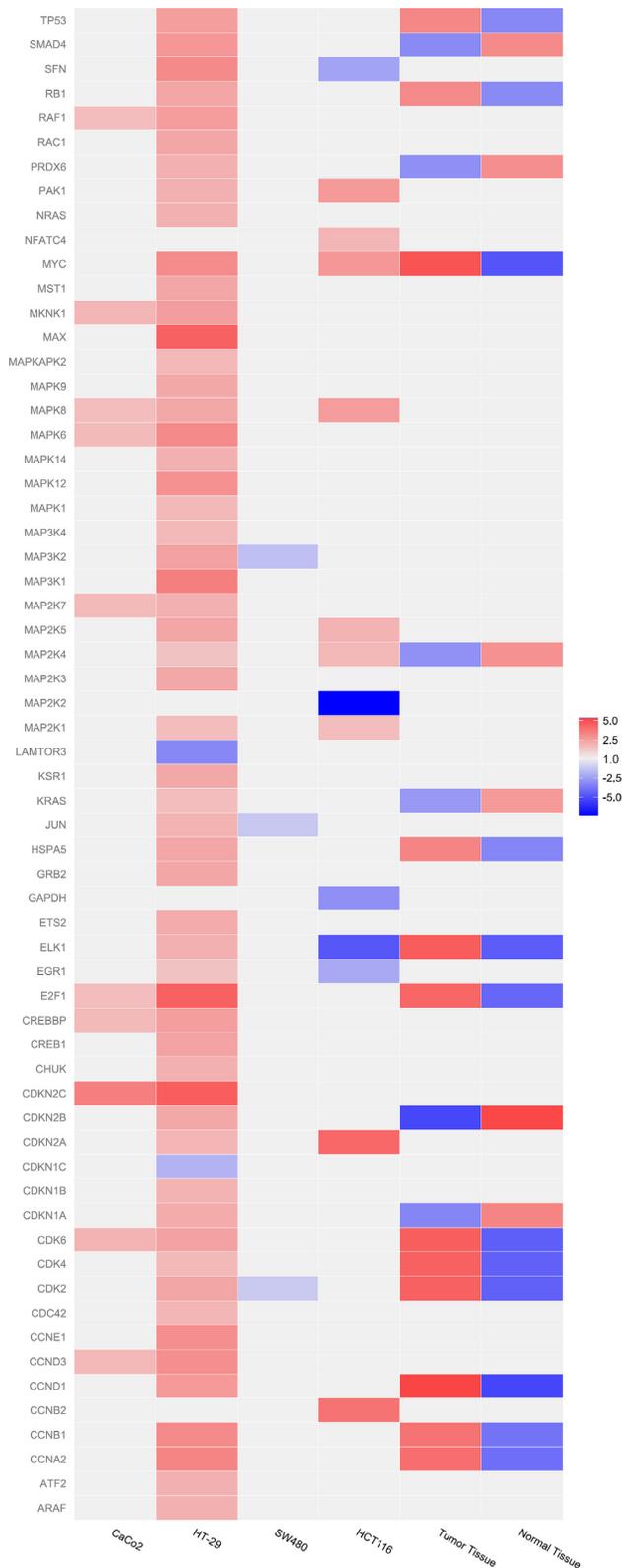
Figure 5. Heatmap of the MAPK signaling pathway genes. Fold change expression data of *MAPK* signaling pathway genes in four colon cancer cell lines after miR-145 ectopic expression. For comparative purposes, gene expression values of matched pairs of tumour and adjacent non-tumorous mucosa samples are also shown.

and especially *TP53* and *MYC* also acted as *intermodular hubs*, because they connected two cohesive clusters, the one made of miR-99a, miR-144 and miR-1275, for which miR-1246 worked as seeding node, and the triangle made up of miR-18b, miR-708 and miR-17, the latter being the seeding node.

The expression level of miR-145 was highly correlated with the above-mentioned clique and triangle and, directly or indirectly, with miR-93, miR-143, miR-18a, miR-23a and miR-23b, miR-31, miR-345, miR26b, miR-185 and miR-20a, thus acting as potent modulator of four *intramodular hubs*, namely *TP53*, *MYC*, *CDK4* and *CDK2*I, and as the genuine actuator of a number of important biological functions and pathways (42–45).

First, miR-145 demonstrated to exert a certain control on the *cell cycle* process through a series of partners: *BCL2, FAS, PPIF, MYC* and *E2F1*. In particular, *MYC* promotes the transcription and E2F1 binds to the promoter region of the polycistronic cluster miR-17∼92 (also known as oncomiR-1), one of the most potent oncogenic clusters, participating to *cell proliferation* and *apoptosis* control (46–50). In particular, miR-145 evidenced a significantly negative causal influence on two of the six members of this cluster, miR-17 and miR-18a. Concomitant lower expression values of miR-145 and miR-18a are prognostic evidences of poor survival, by TCGA data analysis. Notice that *E2F1* exhibits the highest *clustering coefficient* score, confirming its high *sociality* in the whole network. Most of the components of this cluster are directly linked to miR-145 (Figure 3B). The control on cell cycle-related processes by miR-145 is strengthened by its indirect modulation of the expression of miR-21 (Figure 3B) and by the direct control of *CDC25A* and *CDK6* genes (in particular this gene ranked 10th by the *closeness* centrality measure).

Second, miR-145 ectopic expression in CRC cell lines triggered the downstream deregulation of critical genes, a significantly high number of which are closely related to the MAPK signaling pathway. *MYC* is activated by various mitogenic signals, such as WNT, SHH and EGF, via the MAPK/ERK signaling pathway, and in our dataset it was aberrantly expressed. Equally, *ELK1*, which is known to induce the *c-fos* proto-oncogene upon phosphorylation by MAPKs (47), was deregulated in our cell lines, being under the control of miR-143, which in turn correlates with miR-145. *CDK2* regulates G1/S transition and S phase progression in association with cyclin E and A. Its activation is dependent on its localization in the nucleus, which can happen upon the formation of CDK2/MAP Kinase complexes (48). MiR-145 has a double indirect influence on this gene, via the MAPK signaling pathway and because of its negative correlation with miR-18a, of which *CDK2* is a theoretical target. MAPKs are also known to modulate the outcome of SMAD activation by TGF-β. Cross-signaling mechanisms between the SMAD and MAPK pathways take place and affect cell fate in the context of carcinogenesis (49). MiR-145 exerts a double control even on *SMAD4* (module 3), modulating the MAPKs and directly targeting *SMAD4*.

Third, miR-145 was tightly connected with miR-143, in line with the literature. They share numerous target genes involved in various cancer-related events, with both influ-
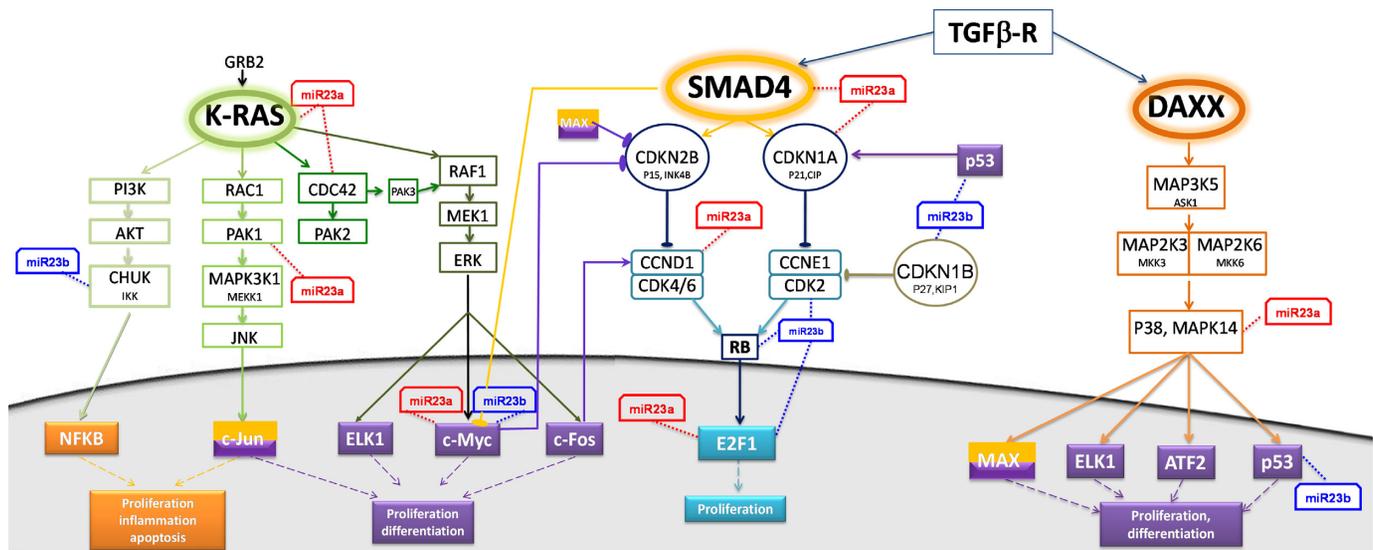
Figure 6. Downstream effects of miR-145 ectopic expression. Pathway map representing the experimental effect points of miR-145 ectopic expression in the HT-29 cell line.

encing phenotypic patterns, as evidenced by experiments entailing the concomitant ectopic expression of the miR-143~miR-145 polycistronic cluster in the HT-29, HCT116 and SW480 cell lines, and showing significant decrease in *proliferation*, *migration*, *anchorage-independent growth* and *chemoresistance*; these miRNAs can work independently or synergistically, with an effect on the colon cancer transcriptome and proteome being characterized by distinct and shared functional effects (50–52). In particular, the miR-143~miR-145 polycistronic cluster targets the RAS-responsive element-binding protein (RREB1) and KRAS (53), which, in turn, induce down-regulation of the cluster, thereby sustaining a feed-forward mechanism (54) that could explain the concurrent down-regulation of KRAS and miR-143~miR-145 cluster in our CRC cohort. From this study, it emerges that it is likely that miR-143 is an effector of miR-145, rather than being equal cooperators. By the analysis of TCGA data comes out that the expression of miR-143 is linearly dependent on miR-145 expression and that the prognosis of patients with low levels of miR-145 and high levels of miR-143 is dismal.

In conclusion, the simultaneous evaluation of the transcriptome and miRNAome of matched pairs of tumour and adjacent non-tumorous mucosa samples of CRC patients helped identifying several modules of genes and miRNAs. A multifaceted enrichment analysis revealed that these modules can cooperate, rather compete, as micro-societies, in the fulfilment of pathophysiological mechanisms underlying the onset and development of CRC. Although several, if not all, members of these clusters could potentially be considered good prognostic and therapeutic targets, many of them, alone, proved to be globally ineffective in the treatment of the disease. For this reason, the hunt for biomarkers shifts attention towards the master-regulators, i.e. the molecules that, when pharmaceutically targeted, can plausibly result in a maximal derangement and destabilization of the core tumour machinery. We focused on miR-145, which, following *in silico* and *in vitro* analysis, demonstrated a high

potential in this direction and could be reliably targeted for diagnostic, prognostic and therapeutic purposes.

ACCESSION NUMBERS

The Array Express accession numbers for mRNA and miRNA expression data are E-MTAB-829 (human tissue), E-MTAB-752 (human tissue) and E-MTAB-2704 (human cell lines).

SUPPLEMENTARY DATA

Supplementary Data are available at NAR Online.

ACKNOWLEDGEMENTS

FUNDING

REFERENCES

1. Kim,V.N. and Nam,J.W. (2006) Genomics of microRNA. *Trends Genet.*, **22**, 165–173.
2. Huntzinger,E. and Izaurralde,E. (2011) Gene silencing by microRNAs: contributions of translational repression and mRNA decay. *Nat. Rev. Genet.*, **12**, 99–110.
3. Calin,G.A., Sevignani,C., Dumitru,C.D., Hyslop,T., Noch,E., Yendamuri,S., Shimizu,M., Rattan,S., Bullrich,F., Negrini,M. *et al.* (2004) Human microRNA genes are frequently located at fragile sites and genomic regions involved in cancers. *Proc. Natl. Acad. Sci. U.S.A.*, **101**, 2999–3004.
4. Calore,F., Lovat,F. and Garofalo,M. (2013) Non-coding RNAs and cancer. *Int. J. Mol. Sci.*, **14**, 17085–17110.
5. Markowitz,S.D. and Bertagnolli,M.M. (2009) Molecular origins of cancer: molecular basis of colorectal cancer. *N. Engl. J. Med.*, **361**, 2449–2460.
6. Tarafa,G., Villanueva,A., Farré,L., Rodríguez,J., Musulén,E., Reyes,G., Seminago,R., Olmedo,E., Paules,A.B., Peinado,M.A. *et al.* (2000) DCC and SMAD4 alterations in human colorectal and pancreatic tumor dissemination. *Oncogene*, **19**, 546–555.
7. Cunningham,D., Atkin,W., Lenz,H.J., Lynch,H.T., Minsky,B., Nordlinger,B. and Starling,N. (2010) Colorectal cancer. *Lancet*, **375**, 1030–1047.
8. Jensen,S.A., Vainer,B., Kruhøffer,M. and Sørensen,J.B. (2009) Microsatellite instability in colorectal cancer and association with thymidylate synthase and dihydropyrimidine dehydrogenase expression. *BMC Cancer*, **20**, e25.
9. Wright,C.M., Dent,O.F., Newland,R.C., Barker,M., Chapuis,P.H., Bokey,E.L., Young,J.P., Leggett,B.A., Jass,J.R. and Macdonald,G.A. (2005) Low level microsatellite instability may be associated with reduced cancer specific survival in sporadic stage C colorectal carcinoma. *Gut*, **54**, 103–108.
10. Pritchard,C.C. and Grady,W.M. (2011) Colorectal cancer molecular biology moves into clinical practice. *Gut*, **60**, 116–129.
11. Polakis,P. (2000) Wnt signaling and cancer. *Genes Dev.*, **14**, 1837–1851.
12. Kobayashi,M., Honma,T., Matsuda,Y., Suzuki,Y., Narisawa,R., Ajioka,Y. and Asakura,H. (2000) Nuclear translocation of beta-catenin in colorectal cancer. *Br. J. Cancer*, **82**, 1689–1693.
13. Huang,K., Zhang,J.X., Han,L., You,Y.P., Jiang,T., Pu,P.Y. and Kang,C.S. (2010) MicroRNA roles in beta-catenin pathway. *Mol. Cancer*, **9**, 252–264.
14. Dhillon,A.S., Hagan,S., Rath,O. and Kolch,W. (2007) MAP kinase signaling pathways in cancer. *Oncogene*, **26**, 3279–3290.
15. Roberts,P.J. and Der,C.J. (2007) Targeting the Raf-MEK-ERK mitogen-activated protein kinase cascade for the treatment of cancer. *Oncogene*, **26**, 3291–3310.
16. Santarpia,L., Lippman,S.M. and El-Naggar,A.K. (2012) Targeting the MAPK-RAS-RAF signaling pathway in cancer therapy. *Exp. Opinion Ther. Targets*, **16**, 103–119.
17. Phipps,A.I., Buchanan,D.D., Makar,K.W., Win,A.K., Baron,J.A., Lindor,N.M., Potter,J.D. and Newcomb,P.A. (2013) KRAS-mutation status in relation to colorectal cancer survival: the joint impact of correlated tumor markers. *Br. J. Cancer*, **108**, 1757–1764.
18. Akao,Y., Nakagawa,Y. and Naoe,T. (2007) MicroRNA-143 and -145 in colon cancer. *DNA Cell Biol.*, **26**, 311–320.
19. Cancer Genome Atlas Network. (2012) Comprehensive molecular characterization of human colon and rectal cancer. *Nature*, **487**, 330–337.
20. Piepoli,A., Tavano,F., Copetti,M., Mazza,T., Palumbo,O., Panza,A., di Mola,F.F., Pazienza,V., Mazzoccoli,G., Biscaglia,G. *et al.* (2012) Mirna expression profiles identify drivers in colorectal and pancreatic cancers. *PLoS One*, **7**, e33663.
21. Caldas,C. and Brenton,J.D. (2005) Sizing up miRNAs as cancer genes. *Nat. Med.*, **11**, 712–714.
22. Hecker,N., Stephan,C., Mollenkopf,H.J., Jung,K., Preissner,R. and Meyer,H.A. (2013) A new algorithm for integrated analysis of miRNA-mRNA interactions based on individual classification reveals insights into bladder cancer. *PloS One*, **8**, e64543.
23. Kim,S.J., Ha,J.W. and Zhang,B.T. (2013) Constructing higher-order miRNA-mRNA interaction networks in prostate cancer via hypergraph-based learning. *BMC Syst. Biol.*, **7**, 47.
24. Mezlini,A.M., Wang,B., Deshwar,A., Morris,Q. and Goldenberg,A. (2013) Identifying cancer specific functionally relevant miRNAs from gene expression and miRNA-to-gene networks using regularized regression. *PLoS One*, **8**, e73168.
25. Piepoli,A., Palmieri,O., Maglietta,R., Panza,A., Cattaneo,E., Latiano,A., Laczko,E., Gentile,A., Carella,M., Mazzoccoli,G. *et al.* (2012) The expression of leucine-rich repeat gene family members in colorectal cancer. *Exp. Biol. Med. (Maywood)*, **237**, 1123–1138.
26. Wu,J., Irizarry,R., MacDonald,J. and Gentry,J. gcrma: background adjustment using sequence information. R package version 2.40.0.
27. Fox,J. (2005) The R Commander: a basic statistics graphical user interface to R. *J. Stat. Softw.*, **14**, 1–42.
28. Kapushesky,M., Adamusiak,T., Burdett,T., Culhane,A., Farne,A., Filippov,A., Holloway,E., Klebanov,A., Kryvych,N., Kurbatova,N. *et al.* (2012) Gene Expression Atlas update - a value-added database of microarray and sequencing-based functional genomics experiments. *Nucleic Acids Res.*, **40**, D1077–D1081.
29. Huang,D.W., Sherman,B.T. and Lempicki,R.A. (2009) Systematic and integrative analysis of large gene lists using DAVID Bioinformatics Resources. *Nat. Protoc.*, **4**, 44–57.
30. Medina,I., Carbonell,J., Pulido,L., Madeira,S.C., Goetz,S., Conesa,A., Tárraga,J., Pascual-Montano,A., Nogales-Cadenas,R., Santoyo,J. *et al.* (2010) Babelomics: an integrative platform for the analysis of transcriptomics, proteomics and genomic data with advanced functional profiling. *Nucleic Acids Res.*, **38**, W210–W213.
31. Alexa,A., Rahnenführer,J. and Lengauer,T. (2006) Improved scoring of functional groups from gene expression data by decorrelating GO graph structure. *Bioinformatics*, **22**, 1600–1607.
32. Chen,J., Bardes,E.E., Aronow,B.J. and Jegga,A.G. (2009) ToppGene Suite for gene list enrichment analysis and candidate gene prioritization. *Nucleic Acids Res.*, **37**, W305–W311.
33. Lu,T.P., Lee,C.Y., Tsai,M.H., Chiu,Y.C., Hsiao,C.K., Lai,L.C. and Chuang,E.Y. (2012) miRSystem: an integrated system for characterizing enriched functions and pathways of microRNA targets. *PLoS One*, **7**, e42390.
34. Li,Y., Qiu,C., Tu,J., Geng,B., Yang,J., Jiang,T. and Cui,Q. (2014) HMDD v2.0: a database for experimentally supported human microRNA and disease associations. *Nucleic Acids Res.*, **42**, D1070–D1074.
35. Mostafavi,S., Ray,D., Warde-Farley,D., Grouios,C. and Morris,Q. (2008) GeneMANIA: a real-time multiple association network integration algorithm for predicting gene function. *Genome Biol.*, **9**, S4.
36. Mazzoccoli,G., Tomanin,R., Mazza,T., D'Avanzo,F., Salvalaio,M., Rigon,L., Zanetti,A., Pazienza,V., Francavilla,M., Giuliani,F. *et al.* (2013) Circadian transcriptome analysis in human fibroblasts from Hunter syndrome and impact of iduronate-2-sulfatase treatment. *BMC Med. Genomics*, **6**, 37.
37. Hansen,D.L., Schneiderman,B. and Smith,M.A. (2011) *Analyzing social media networks with NodeXL: insights from a connected world.* Morgan Kaufmann, Burlington.
38. Saito,R., Smoot,M.E., Ono,K., Ruscheinski,J., Wang,P.L., Lotia,S., Pico,A.R., Bader,G.D. and Ideker,T. (2012) A travel guide to Cytoscape plugins. *Nat. Methods*, **9**, 1069–1076.
39. Nepusz,T., Yu,H. and Paccanaro,A. (2012) Detecting overlapping protein complexes in protein-protein interaction networks. *Nat. Methods*, **9**, 471–472.
40. Panza,A., Votino,C., Gentile,A, Valvanom,M.R., Colangelo,T., Pancione,M., Micale,L., Merla,G., Andriulli,A., Sabatino,L. *et al.* (2014) Peroxisome proliferator-activated receptor γ-mediated induction of microRNA-145 opposes tumor phenotype in colorectal cancer. *Biochim. Biophys. Acta*, **1843**, 1225–1236.
41. Liang,H. and Li,W.H. (2007) MicroRNA regulation of human protein protein interaction network. *RNA*, **13**, 1402–1408.
42. Mogilyansky,E. and Rigoutsos,I. (2013) The miR-17/92 cluster: a comprehensive update on its genomics, genetics, functions and increasingly important and numerous roles in health and disease. *Cell Death Differ.*, **20**, 1603–1614.
43. Olive,V., Jiang,I. and He,L. (2010) mir-17-92, a cluster of miRNAs in the midst of the cancer network. *Int. J. Biochem. Cell Biol.*, **42**, 1348–1354.
44. Schulte,J.H., Horn,S., Otto,T., Samans,B., Heukamp,L.C., Eilers,U.C., Krause,M., Astrahantseff,K., Klein-Hitpass,L.,

Buettner,R. *et al.* (2008) MYCN regulates oncogenic MicroRNAs in neuroblastoma. *IJC*, **122**, 699–704.

45. Sylvestre,Y., De Guire,V., Querido,E., Mukhopadhyay,U.K., Bourdeau,V., Major,F., Ferbeyre,G. and Chartrand,P. (2007) An E2F/miR-20a autoregulatory feedback loop. *J. Biol. Chem.*, **282**, 2135–2143.

46. Woods,K., Thomson,J.M. and Hammond,S.M. (2007) Direct regulation of an oncogenic micro-RNAcluster by E2F transcription factors. *J. Biol. Chem.* **282**, 2130–2134.

47. Hipskind,R.A., Rao,V.N., Mueller,C.G., Reddy,E.S and Nordheim,A. (1991) Ets-related protein Elk-1 is homologous to the c-fos regulatory factor p62TCF. *Nature*, **354**, 531–534.

48. Blanchard,D.A., Mouhamad,S., Auffredou,M.T, Pesty,A., Bertoglio,J., Leca,G. and Vazquez,A. (2000) Cdk2 associates with MAP kinase in vivo and its nuclear translocation is dependent on MAP kinase activation in IL-2-dependent Kit 225 T lymphocytes. *Oncogene.*, **19**, 4184–4189.

49. Javelaud,D. and Mauviel,A. (2005) Crosstalk mechanisms between the mitogen-activated protein kinase pathways and Smad signaling downstream of TGF-beta: implications for carcinogenesis. *Oncogene*, **24**, 5742–5750.

50. Akao,Y., Nakagawa,Y. and Naoe,T. (2006) MicroRNAs 143 and 145 are possible common onco-microRNAs in human cancers. *Oncol. Rep.*, **16**, 845–850.

51. Pagliuca,A., Valvo,C., Fabrizi,E., di Martino,S., Biffoni,M., Runci,D., Forte,S., De Maria,R. and Ricci-Vitiani,L. (2013) Analysis of the combined action of miR-143 and miR-145 on oncogenic pathways in colorectal cancer cells reveals a coordinate program of gene repression. *Oncogene*, **32**, 4806–4813.

52. Bauer,K.M. and Hummon,A.B. (2012) Effects of the miR-143/-145 microRNA cluster on the colon cancer proteome and transcriptome. *J. Proteome Res.*, **11**, 4744–4754.

53. Chen,X., Guo,X., Zhang,H., Xiang,Y., Chen,J., Yin,Y., Cai,X., Wang,K., Wang,G., Ba,Y. *et al.* (2009) Role of miR-143 targeting KRAS in colorectal tumorigenesis. *Oncogene*, **28**, 1385–1392.

54. Kent,O.A., Chivukula,R.R., Mullendore,M., Wentzel,E.A., Feldmann,G., Lee,K.H., Liu,S., Leach,S.D., Maitra,A. and Mendell,J.T. (2010) Repression of the miR-143/145 cluster by oncogenic Ras initiates a tumor-promoting feed-forward pathway. *Genes Dev.*, **24**, 2754–2759.